Proceedings of the
International Conference on Mechanical Engineering 2007
(ICME2007) 29- 31 December 2007, Dhaka, Bangladesh

ICME07-AM-75

INVESTIGATION OF FIBER DIAMETER AND INTERPHASE EFFECTS ON THE TENSILE ELASTIC MODULUS OF CARBON NANOTUBE REINFORCED COMPOSITE

A. K. M. Masud[1], **S. C. Chowdhury**[2] **and Abdullah-Al-Khaled**[3]

[1,3] Department of Industrial & Production Engineering, BUET, Dhaka-1000, Bangladesh.
[2]Assistant Professor, Department of Mechanical Engineering, BUET, Dhaka-1000, Bangladesh.

ABSTRACT

In this paper, the effects of nanotube diameter, interphase thickness, and stiffness on the tensile elastic modulus (TEM) of the carbon nanotube (CNT) reinforced composite is investigated using a 3-D nanoscale representative volume element (RVE) based on continuum mechanics and using the finite element method (FEM). Formula to extract the effective material constant from solutions for the RVE under axial loading is derived based on the elasticity theory. Both long and short CNT embedded in the matrix at volume fraction of 5% and 2.5% respectively are considered. First, we investigate the effects of CNT diameter on the TEM of the composite. Numerical results show that in case of short CNT, influence of tube diameter on the TEM of the composite is significant. Then we investigate the effect of interphase thickness for both soft interphase/stiff matrix and stiff interphase/soft matrix combination, and the effect of interphase stiffness at a particular thickness of interphase on the TEM of composite. Results show that both the thickness and stiffeness of the interphase significantly influence the TEM of the composite.

Keywords: Carbon nanotube, Composite, Elastic modulus, FEM.

1. INTRODUCTION

Nanocomposites, based on carbon nanotubes (CNTs), have attracted great interest since their discovery by Iijima in 1991 [1]. Recent theoretical calculations and direct experimental measurements showed that the elastic modulus of a CNT is in the range of 1-5 TPa [2-4], which is significantly higher than that of a carbon fiber, from 0.1 to 0.8 TPa [5]. Such superior mechanical properties make CNTs to possess exceptionally high stiffness, strength and resilience. At the same time, they also possess superior electrical and thermal properties [6]. The mechanical load carrying capacities of CNTs in nanocomposites have also been demonstrated in some experimental work [7-10] and numerical simulations [6]. All these investigations show that the load-carrying capacity of CNTs in a matrix is significant and the CNT-based composites have the potential to provide extremely strong and ultralight new materials [11]. However, the degree of reinforcement observed in different experiments [7-10] differs significantly. Therefore, it is necessary to investigate which factors influence on the reinforcement of the CNT based composites.

Computational approach can play a significant role in the development of the CNT-based composites by providing simulation results to help on the understanding, analysis and design of such nanocomposites. At the nanoscale, analytical models are difficult to establish or too complicated to solve, and tests are extremely difficult and expensive to conduct. Modeling and simulations of nanocomposites, on the other hand, can be achieved readily and cost effectively on even a desktop computer. Characterizing the mechanical properties of CNT-based composites is just one of the many important and urgent tasks that simulations can accomplish.

In this paper, the effective tensile elastic modulus (TEM) of CNT-based composites is evaluated using a 3-D nanoscale representative volume element (RVE) based on continuum mechanics and using the finite element method (FEM). Using this formula and the output from FEM, the effect of the variation in nanotube diameter in the nanocomposite, for both long and short fiber at about 5% and 2.5% volume fraction respectively, on the TEM of nanocomposite is investigated. Then it is also observed that an interphase is unavoidable in the production of composites and can form in a number of ways [12], for example:

(1) The presence of adsorbed contaminants on the fiber surface, which are not adsorbed during impregnation and cure;

(2) Diffusion of chemical species to the interface between fiber and matrix;

(3) Acceleration or retardation of polymerization at he interface;

(4) The deliberate inclusion of sizing resin at the time of fiber manufacture.

The effect of an interphase on the performance of the composite is not well characterized, since its precise nature is difficult to predict [13]. Scanning probe microscopy (SPM) [14-16] has been used to examine the mechanical and thermal properties in the immediate vicinity of reinforcing fibers. In this way, it has been clearly shown that sized reinforcing fibers modify the properties of the matrix. In this paper, the effects of interphase thickness for both soft interphase/stiff matrix and stiff interphase/soft matrix combination, and interphase stiffness at a particular thickness of the interphase on the TEM of the nanocomposites have also been investigated. The investigations are carried out for long and short CNT.

The organization of this paper is as follows. Cylindrical RVEs, used in this paper, for both short and long CNTs, are discussed in Section 2. Formulas based on the elasticity theory to extract the material constants from numerical analysis are derived in Section 3. Finite element analyses of the RVEs and results are presented in Section 4. Finally, discussions and conclusions are offered in Section 5.

2. RVE FOR EVALUATIONS OF THE EFFECTIVE MATERIAL PROPERTIES

CNTs are in different sizes and forms when they are dispersed in a matrix to make a nanocomposite. They can be single-walled or multi-walled with length of a few nanometers or a few micrometers, and can be straight, twisted and curled, or in the form of ropes [17]. Their distribution and orientation in the matrix can be uniform and unidirectional (which may be the ultimate goal) or random. All these factors make the simulations of CNT-based composites extremely difficult. To start with, the concept of unit cells or representative volume elements, which have been applied successfully in the studies of conventional fiber-reinforced composites at the microscale [18], can be extended to study the CNT-based composites at the nanoscale. In this RVE approach, a single (or multiple) nanotube(s) with surrounding matrix material can be modeled, with properly applied boundary and interface conditions to account for the effects of the surrounding materials. Numerical methods, such as the FEM, boundary element method or mesh free method can be applied to analyze the mechanical responses of these RVEs under different loading conditions.

Interfaces between the CNTs and matrix are crucial regions to ensure the load carrying capacity and other functionalities of the nanocomposites. They are also the most difficult regions for any simulation approaches. To start with, perfect bonding can be assumed between the CNTs and matrix in the continuum mechanics models of CNT-based composites [6]. Research has demonstrated that the possibility of such a strong (C–C) bond exists for CNT-based composites [17].

In this paper, the cylindrical RVE, shown in Fig. 1 (for long CNT) and Fig. 2 (for short CNT), are employed to evaluate the effective TEM of the CNT-based composites. The required mathematical results used to extract the material constant from the simulation results (by using the FEM) are established in the next section.

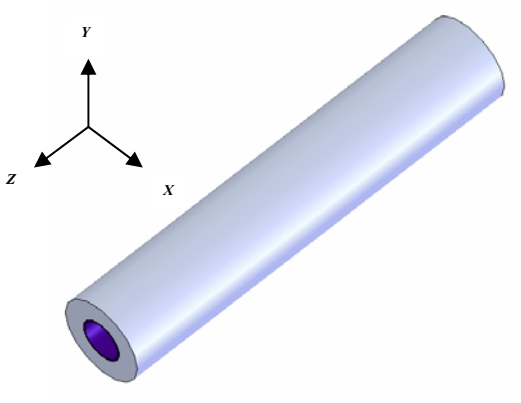

Fig 1: The cylindrical RVE containing long fiber.

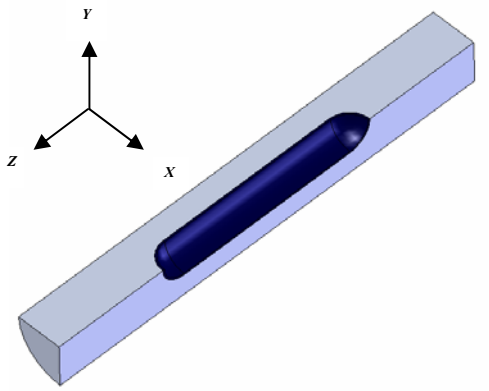

Fig 2: The quarter cylindrical RVE containing short fiber.

3. FORMULAS FOR EVALUATIONS OF THE EFFECTIVE MATERIAL CONSTANTS

It is assumed that both the CNTs and matrix in a RVE are continua of linearly elastic, isotropic and homogenous materials, with given Young's moduli and Poisson's ratios. The RVE can contain one CNT (Fig. 1 & 2) or multiple CNTs, determined by the main criterion that it should be large enough to be representative of the material and small enough to be modeled and analyzed efficiently using a solution method. Under the above assumptions, there will be two effective material constants to be determined for the CNT-based composite, namely, one Young's modulus E_x (= E_y = E_z) and one Poisson's ratio ν_{xy} (= ν_{zx} = ν_{zy}) (see Fig. 1 & 2 for the orientation of the coordinates).

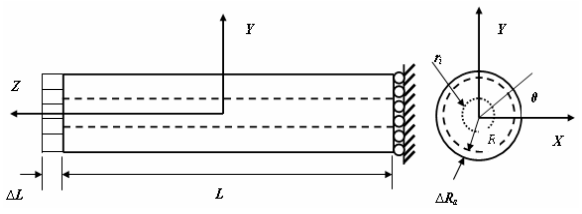

Fig 3: The cylindrical RVE used to evaluate the TEM of the CNT-based composites under axial stretch ΔL.

To derive the formula for extracting the TEM, a homogenized elasticity model corresponding to the RVE

is considered. The geometry of the elasticity model is corresponding to a hollow cylindrical RVE with length L, inner radius r_i and outer radius R (Fig. 3), so that analytical solutions can be obtained. This geometry can account for the cases when the CNT is relatively long and thus all the way through the length of the RVE. In the case that the CNT is relatively short and thus fully inside the RVE, a solid cylindrical RVE ($r_i = 0$) can be used for extracting the material constant, since the elasticity solutions are difficult to find in this case. The material of the elasticity model, considered in this paper, is isotropic and the general 3-D strain–stress relations are given by

$$\begin{Bmatrix} \varepsilon_x \\ \varepsilon_y \\ \varepsilon_z \end{Bmatrix} = \begin{bmatrix} \frac{1}{E_x} & -\frac{\nu_{xy}}{E_x} & -\frac{\nu_{xy}}{E_x} \\ -\frac{\nu_{xy}}{E_x} & \frac{1}{E_x} & -\frac{\nu_{xy}}{E_x} \\ -\frac{\nu_{xy}}{E_x} & -\frac{\nu_{xy}}{E_x} & \frac{1}{E_x} \end{bmatrix} \begin{Bmatrix} \sigma_x \\ \sigma_y \\ \sigma_z \end{Bmatrix} \quad (1)$$

in the (*x, y, z*) coordinates shown in Fig. 1 & 2. This relation is also valid for the stress and strain components in the cylindrical coordinate system (*r, θ, z*) (Fig. 3).

For the axial loading, shown in Fig. 3, the stress and strain components at any point on the lateral surface are

$$\sigma_x = \sigma_y = \sigma_r = \sigma_\theta = 0,$$

$$\varepsilon_z = \frac{\Delta L}{L}, \varepsilon_\theta = \frac{\Delta R_a}{R}, \text{ with } \Delta R_a < 0, \text{ if } \Delta L > 0,$$

where ΔR_a is the radial displacement, and r and θ indicate the radial and tangential components in the polar coordinate system, respectively. From Eq. (1), one has immediately

$$E_x = E_z = \frac{\sigma_z}{\varepsilon_z} = \frac{L}{\Delta L}\sigma_{ave} \quad (2)$$

where the averaged stress is given by

$$\sigma_{ave} = \frac{1}{A}\int_A \sigma_z(x, y, L/2)dxdy,$$

with A being the area of the end surface. σ_{ave} can be evaluated for the RVE using the FEM results.

4. FINITE ELEMENT MODELING AND RESULTS

To evaluate the effective TEM of CNT-based nanocomposite, the cylindrical RVE (Fig. 1 & 2) for a single-walled carbon nanotube in a matrix material is studied using the finite element method. The model is created using ANSYS 10.0. The deformations and stresses are computed first for the axial loading (Fig. 3) described in Section 3. The FEM results are then processed, and Eq. (2) is applied to extract the effective TEM for the CNT-based composite. Three effects are studied, with the RVE for both long and short CNT. In all the cases, axisymmetric FEM models are used since the RVEs have an axisymmetric geometry and the loading is also axisymmetric (Fig. 3). So, this case can be handled by axisymmetric FEM model. The models are meshed using quadratic (8-node) ring elements (type Plane 82), which are second order elements and offer better accuracy in stress analysis and axisymmetric boundary conditions are employed.

4.1 Effect of Nanotube Diameter Variation on the TEM of Nanocomposite

The RVEs for long CNT all the way through the RVE length, as shown in Fig. 1, are studied. The volume fraction of the CNT is kept constant for all the models, which is about 5%. The length of the matrix and CNT is kept constant, which is, L = 100 nm and the effective thickness of the CNT is kept 0.4 nm. The inner radius (r_i), outer radius (r_o) of the CNT and the radius (R) of the matrix are given in Table 1. It can be mentioned here that these CNT radii (shown in Table 1) are of the armchair tubules with indices of (50, 50), (70, 70), (80, 80), (110, 110), (130, 130) and (150, 150) respectively.

Table 1: The radii of CNT and matrix

R (nm)	r_o (nm)	r_i (nm)
8.04	3.6	3.2
9.83	4.95	4.55
10.65	5.6	5.2
13.2	7.7	7.3
14.65	9	8.6
16.2	10.4	10

The Young's modulus and Poisson's ratios used for the CNT and matrix are:
CNT: $E_t = 1000$ GPa, $\nu_t = 0.3$;
Matrix: $E_m = 100$ GPa, $\nu_m = 0.3$;
The finite element mesh used is shown in Fig. 4.

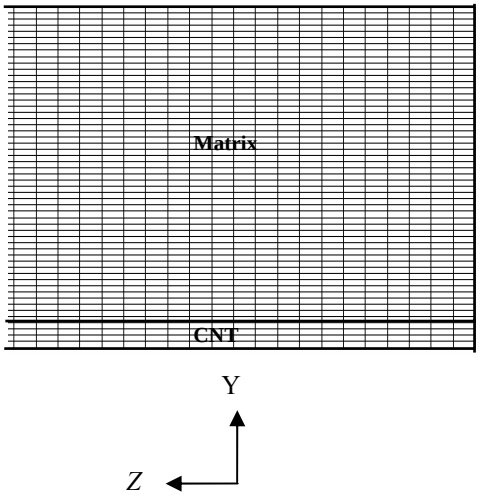

Fig 4: Partial view of the axisymmetric FEM model for the RVE with long CNT (the element size is 0.2 nm by 0.4 nm).

Two layers of elements are used for the CNT in this mesh which is found to be fine enough to deliver converged FEM results. The FEM model is loaded in the axial direction as shown in Fig. 3. The TEM, E_z of the composite is extracted from Eq. (2) using the FEM results. The FEM result for the effective material constant (i.e. TEM) of the CNT-based composite for long

fiber studied is shown in Fig 5. It is seen that for long CNT, tube diameter has negligible effect on the effective TEM of the composite.

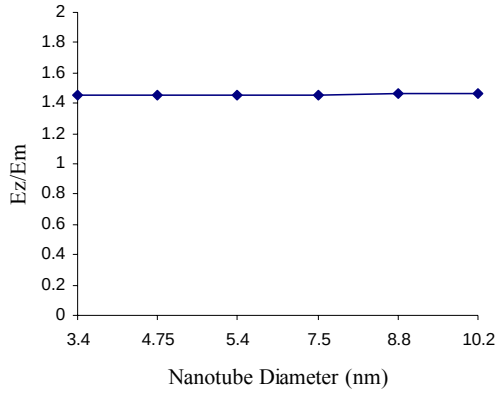

Fig 5: Effect of the variation of nanotube diameter on the TEM of the matrix containing long CNT.

The stress contour plot of the first principal stresses in the RVE, with 5.4 nm of CNT diameter, under the axial stretch is shown in Fig. 6.

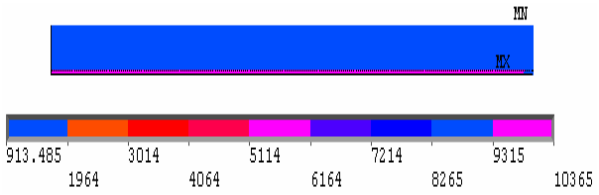

Fig 6: Plot of the first principal stresses for the long CNT-based model under the axial stretch (E_t/E_m = 10).

Next, the RVEs with short CNT, as shown in Fig. 2, are studied. The volume fraction of the CNT is kept constant for all the models with the short CNT, which is 2.5%. The length of the matrix is kept equal to model with long CNT (L = 100 nm) and the CNT total length is reduced to 50 nm (with the two hemispherical end caps) and also the effective thickness of the CNT is taken 0.4 nm. The inner radius (r_i), outer radius (r_o) of the CNT and the radius (R) of the matrix are given in Table 2.

Table 2: The radii of CNT and matrix

R (nm)	$\mathbf{r_o}$ (nm)	$\mathbf{r_i}$ (nm)
3.4	3.6	3.2
4.75	4.95	4.55
6.1	6.3	5.9
7.5	7.7	7.3

Here, the CNT radii (shown in Table 2) are taken of the armchair tubules with indices of (50, 50), (70, 70), (90, 90) and (110, 110) respectively.

The Young's modulus and Poisson's ratios used for CNT and matrix are same as the RVE with long CNT.

The finite element mesh used is shown in Fig. 7.

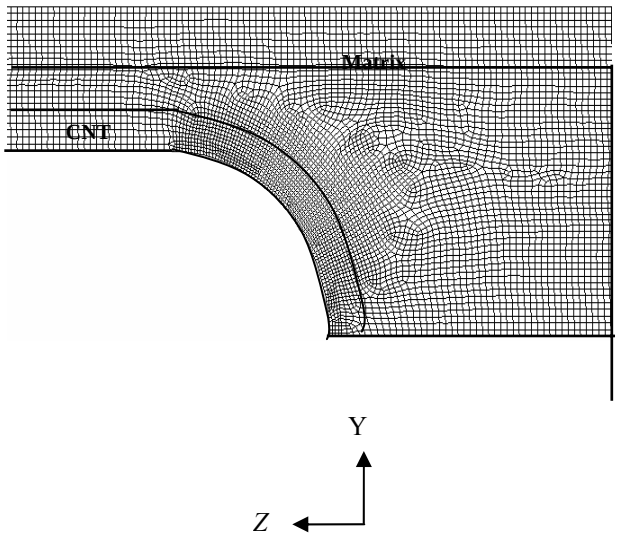

Fig 7: Partial view of the axisymmetric FEM model for the RVE with short CNT (the element size is 0.1 nm by 0.2 nm).

The FEM results for the effective TEM of the CNT-based composite for short CNT studied are shown in Fig. 8, which shows that for short CNT, tube diameter significantly influences the TEM of the composite.

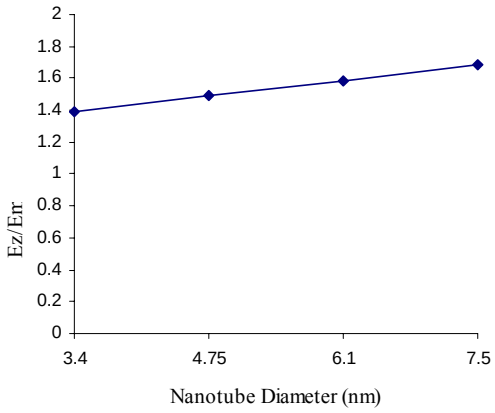

Fig 8: Effect of the variation of nanotube diameter on the TEM of the matrix containing short CNT.

The stress contour plot of the first principal stresses in the RVE, with 5.4 nm of CNT diameter, under the axial stretch is shown in Fig. 9.

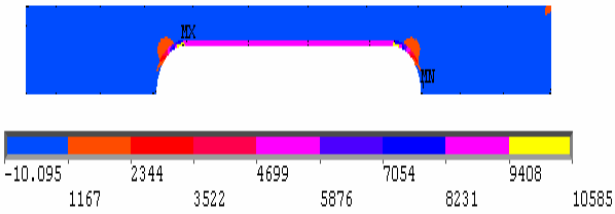

Fig 9: Plot of the first principal stresses for the short CNT-based model under the axial stretch (E_t/E_m = 10).

4.2 Effect of the Variation of Interphase Thickness on the TEM of nanocomposite

In investigating the RVEs for long CNT, with interphase of various thicknesses, the length of the matrix and CNT are kept constant as in Section 4.1 (RVE for long CNT), and the CNT radius is taken with the index of (80, 80), which dimensions are given in Table 1. So, the radius (R) of the matrix is taken as 10.65 nm at 5% volume fraction of CNT. The thicknesses of interphase are considered as 0 nm (*i.e.* without interphase) 0.2 nm, 1.5 nm, 2.1 nm and 3 nm respectively. Two interphase properties are considered; one is soft interphase and the other is stiff interphase compared to matrix which is justified in [13]. The Young's modulus and Poisson's ratios used for the CNT, Interphase and matrix are:

CNT: $E_t = 1000$ GPa, $\nu_t = 0.3$;
Interphase: $E_i = 200$ GPa (Stiff) and 20 GPa (Soft), $\nu_i = 0.3$
Matrix: $E_m = 100$ GPa, $\nu_m = 0.3$;

The FEM results, for the variation of interphase thickness are shown in Fig 10. It is found that for stiff interphase composite modulus increases with the increase of interphase thickness whereas for soft interphase composite modulus decreases with the increase of the interphase thickness.

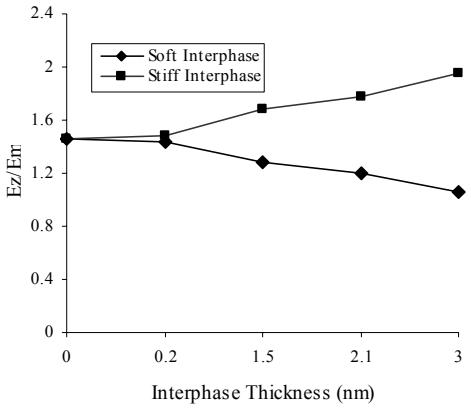

Fig 10: Effects of the variation of interphase thickness on the TEM of the matrix containing long CNT.

The stress contour plot of the first principal stresses in the RVE, with 1.5 nm interphase thickness, under the axial stretch is shown in Fig. 11.

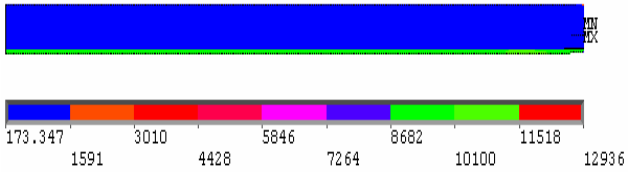

Fig 11: Plot of the first principal stresses for the RVE (long CNT) with interphase under axial stretch (E_t/E_m = 10).

Next, in investigating the RVEs for short CNT, with interphase of various thicknesses, the length of the matrix and CNT are kept constant as in Section 4.1 (RVE for short CNT) and the CNT radius is taken with the index of (80, 80), which dimensions are: $r_o = 5.6$ nm and $r_i = 5.2$ nm and the radius (R) of the matrix is taken as 9.252 nm at 2.5% volume fraction CNT. The thicknesses of interphase are considered as 0 nm (i.e. without interphase) 0.2 nm, 1.5 nm, 2.1 nm and 3 nm respectively. Again, two interphase properties are considered; one with soft interphase and the other with stiff interphase compared to matrix.

The Young's modulus and Poisson's ratios used for the CNT, Interphase and matrix are considered same as mentioned above in this Section 4.2.

The FEM results, for the variation of interphase thickness are shown in Fig 12. For short CNT, the trend of variation of the composite modulus with interphase thickness and stiffness is the same as long CNT.

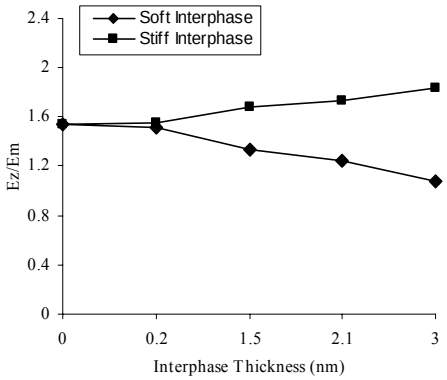

Fig 12: Effects of the variation of interphase thickness on the TEM of the matrix containing short CNT.

The stress contour plot of the first principal stresses in the RVE, with 1.5 nm interphase thickness, under the axial stretch is shown in Fig. 13.

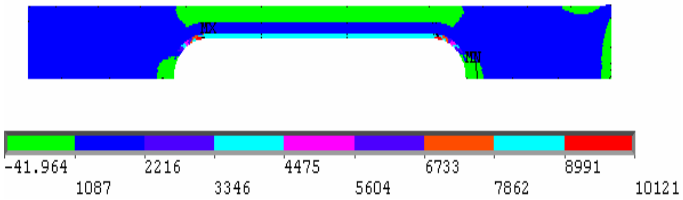

Fig 13: Plot of the first principal stresses for the RVE (short CNT) with interphase under axial stretch (E_t/E_m = 10).

4.3 Effect of the Variation of Interphase Stiffness on the TEM of Nanocomposite

In studying the effect of change in interphase stiffness, the dimensions of RVE with long CNT are considered as R = 10.65 nm, $r_o = 5.2$ nm and $r_i = 4.6$ nm, with the thickness of interphase as 1.5 nm.

Again, for RVE with short CNT, the dimensions are considered as R = 9.252 nm, $r_o = 5.2$ nm and $r_i = 4.6$ nm, with the thickness of interphase as 1.5 nm. The FEM results for both long and short CNT-based composite is shown in Fig 14. It is seen that for both types of CNT,

composite modulus increases with the increase of interphase stiffness.

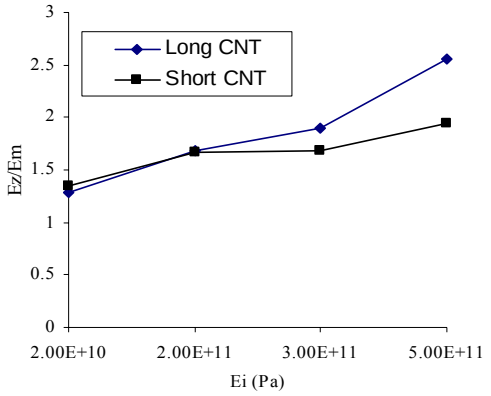

Fig 14: Effects of the variation of interphase stiffness on the TEM of the CNT-based composite.

5. CONCLUSIONS

The effects of nanotube diameter, interphase thickness and stiffness on the tensile elastic modulus of the carbon nanotube (CNT) reinforced composite is investigated using a 3-D nanoscale representative volume element (RVE) based on continuum mechanics and using the finite element method (FEM). Effective material constant (i.e., modulus) of the composite is determined from the solutions of the RVE under axial loading using the elasticity theory. Both long and short CNT at volume fraction of 5% and 2.5% respectively are considered. From the numerical results, the following conclusions are obtained.

(1) For long CNT based composite, tube diameter has negligible effect on the tensile elastic modulus of the composite.

(2) For short CNT based composite, tube diameter significantly influences the tensile elastic modulus of the composite.

(3) Composite modulus increases with the increase of interphase thickness for stiff interphase whereas for soft interphase composite modulus decreases with the increase of the interphase thickness.

(4) Composite modulus increases with the increase of interphase stiffness.

6. REFERENCES

1. Iijima, S., 1991, "Helical Microtubules Graphite Carbon", Nature, 354: 56-58.
2. Treacy, M. M., Ebbesen, T. W., and Gibson, J. M., 1996, Nature, 381: 678.
3. Wong, E.W., Sheehan, P. E., and Lieber, C. M., 1997, Science, 277: 1971.
4. Zhang, P., Huang, Y., Geubelle, P. H., Klein, P. A., Hwang, K. C., 2002, International Journal of Solids and Structures, 39: 3893.
5. Peebles, L. H., 1995, "Carbon Fibers: Formation, Structure and Properties" CRC Press, Boca Raton.
6. Liu, Y.J. and Chen, X.L., 2003, "Evaluations of the Effective Materials Properties of Carbon Nanotube-Based Composites Using a Nanoscale Representative Volume Element", Mechanics of Materials, 35: 69–81.
7. Qian, D., Dickey, E.C., Andrews, R. and Rantell, T., 2000, "Load Transfer and Deformation Mechanisms in Carbon Nanotube–Polystyrene Composites", Applied Physics Letters, 76: 2868–2870.
8. Wagner, H.D., Lourie, O., Feldman, Y. and Tenne, R., 1998, "Stress Induced Fragmentation of Multiwall Carbon Nanotubes in a Polymer Matrix", Applied Physics Letters, 72: 188–190.
9. Schadler, L.S., Giannaris, S.C. and Ajayan, P.M., 1998, "Load Transfer in Carbon Nanotube Epoxy Composites", Applied Physics Letters, 73: 3842–3844.
10. Bower, C., Rosen, R., Jin, L., Han, J., Zhou, O., 1999, "Deformation of Carbon Nanotubes in Nanotube–Polymer Composites", Applied Physics Letters 74: 3317–3319.
11. Chen, X.L. and Liu Y.J., 2004, "Square Representative Volume Elements for Evaluating the Effective Material Properties of Carbon Nanotube-Based Composites", Computational Materials Science 29: 1–11.
12. Jones, F. R., 1996, "Interphase Formation and Control in Fiber Composite Materials", Key EngNg Mater, 116/117: 41-60.
13. Hayes, S. A., Lane, R., and Jones, F. R., 2001, "Fibre/Matrix Stress Transfer Through a Discrete Interphase. Part 1: Single-Fibre Model Composites" Composites: Part A, 32: 379-389.
14. Mai, K., Maider, E., and Muhle, M., 1998, "Interphase Characterisation in Composites, With New Non-Destructive Methods", Composites: Part-A, 29: 1111-1119.
15. Munz, M., Strum, H., Sculz, E. and Hinrichsen, G., 1998, "The Scanning Force Microscope as a tool for the detection of local Mechanical Properties Within the Interphase of Fiber Reinforced Polymers", Composites: Part-A, 29: 1251-1259.
16. Landingham, M. R., Dagastine, R. R., Eduljee, R. F., McCullogh, R. L., and Gillespie, J. W., 1999, "Characterisation of Nanoscale Property Variations in Polymer Composite Systems: 1. Experimental Results" Composites: Part- A, 90: 75-83.
17. Thostenson, E. T., Ren, Z. F. and Chou, T. W., 2001, "Advances in the Science and Technology of Carbon Nanotubes and Their Composites: A Review", Composites Science and Technology 61, 1899-1912.
18. Hyer, M. W., 1998, "Stress Analysis of Fiber-Reinforced Composite Materials" McGraw-Hill, Boston.

7. NOMENCLATURE

Symbol	Meaning	Unit
E	Young's Modulus	(Pa)
ν	Poisson's Ratio	
σ	Stress	(Pa)
ε	Strain	